Analysis of the Structure and Resolution of a Graphics Device

P. A. FIRBY AND D. J. STONE

Department of Mathematics, University of Exeter, Exeter, Devon EX4 4QE, UK

It is shown how a graphics device can be given pictures to display which reveal its own underlying structure, its dimensions and its faults.

Received March 1994; revised May 1994

1. INTRODUCTION

Superimposed periodic patterns often produce interference. The interference caused by superimposed families of curves was studied in general form by Firby and Hubbard (1990). The approach used there, and used again in this current paper, is that of simple spatial domain mathematics. Other approaches to the analysis of interference are possible as can be seen in Bryngdahl (1976), Harthong (1981) or in Kendig (1980).

An analysis of the interference of direct relevance to the process of printing appeared in Tollenaar (1957), in Steinbach and Wong (1979) and more recently in Amidror (1991).

Here we consider the application of the ideas of interference to the practical problem of analysing the presented structure and the resolution of a graphics device.

2. DETERMINING THE STRUCTURE

In covering a plane area by dots or pixels we can assume two independent translations are in operation. The pattern produced can then be interpreted in terms of two-dimensional crystallography and the array produced by the centres of the dots or pixels will be the associated two-dimensional lattice.

It is known that the only possible periods for a rotational symmetry operation of a two-dimensional lattice are 2, 3, 4, and 6 (Coxeter, 1969; Hoggar, 1992). Examples of two-dimensional lattices with periods 2, 4 and 6 are shown in Figure 1(a–c), and we note that a family of parallel lines, as shown in Figure 1(d), has period 2.

Suppose a lattice L_1 with period n_1 is superimposed on a lattice L_2 with period n_2, and then the whole picture is rotated. The lattice L_1 will regain its initial configuration n_1 times within 2π, while L_2 will regain its initial configuration n_2 times. It follows that the full picture will regain its initial configuration n times within 2π, where n is the greatest common divisor of n_1 and n_2.

Thus if two lattices of the form shown in Figure 1(c), each of period 6, are superimposed then the resulting picture will again have period 6. This is shown in Figure 2(a). However, if a lattice of the form shown in Figure 1(c), with period 6, is superimposed on a lattice of the form shown in Figure 1(b), with period 4, then the resulting picture will have period 2. This is illustrated in Figure 2(b). Similarly a lattice of the form shown in Figure 1(a) superimposed on a lattice of the form shown in Figure 1(b), will produce a picture of the type shown in Figure 2(c), with period 2. In each case the superimposed lattice has been slightly rotated to bring out the interference.

Now when a picture is presented on a monitor or on a printer the process involved is better described as a composition of two functions. Instead of the picture being superimposed on the underlying structure of the device it is filtered through this underlying structure. However, the same principles apply. The centres of the pixels or dots form an underlying two-dimensional lattice. If the Dirichlet region of a point in this lattice has non-empty intersection with the picture then the associated pixel or point is 'switched on'. Then if the underlying two-dimensional lattice has rotational period n_1 and the picture has period n_2 the observed picture will have period $n = gcd(n_1, n_2)$.

Using these ideas we can ask a visual devise to 'analyse its own structure' by presenting suitable pictures.

Figure 3(a) shows what happens when a console is asked to present a picture of a two-dimensional lattice with suitable spacing and with period 6, of the form shown in Figure 1(c). The observed picture has period 2 from which we deduce that the underlying pixel structure cannot have period 3 or 6. Figure 3(b) shows what happens when the same console is asked to present a picture of a two-dimensional lattice of period 4 of the form shown in Figure 1(b) but slightly rotated. The observed picture has period 2 from which we deduce that the underlying pixel structure has period 2. Moreover the observed picture has the form of Figure 2(c). The dots in the square lattice are evidently interfering with horizontal sequences of pixels and vertical sequences of pixels in the underlying structure to produce the sides of the parallelograms. We are led to the conclusion that the two-dimensional lattice associated with the underlying pixel structure is a rectangular lattice similar to that shown in Figure 1(a).

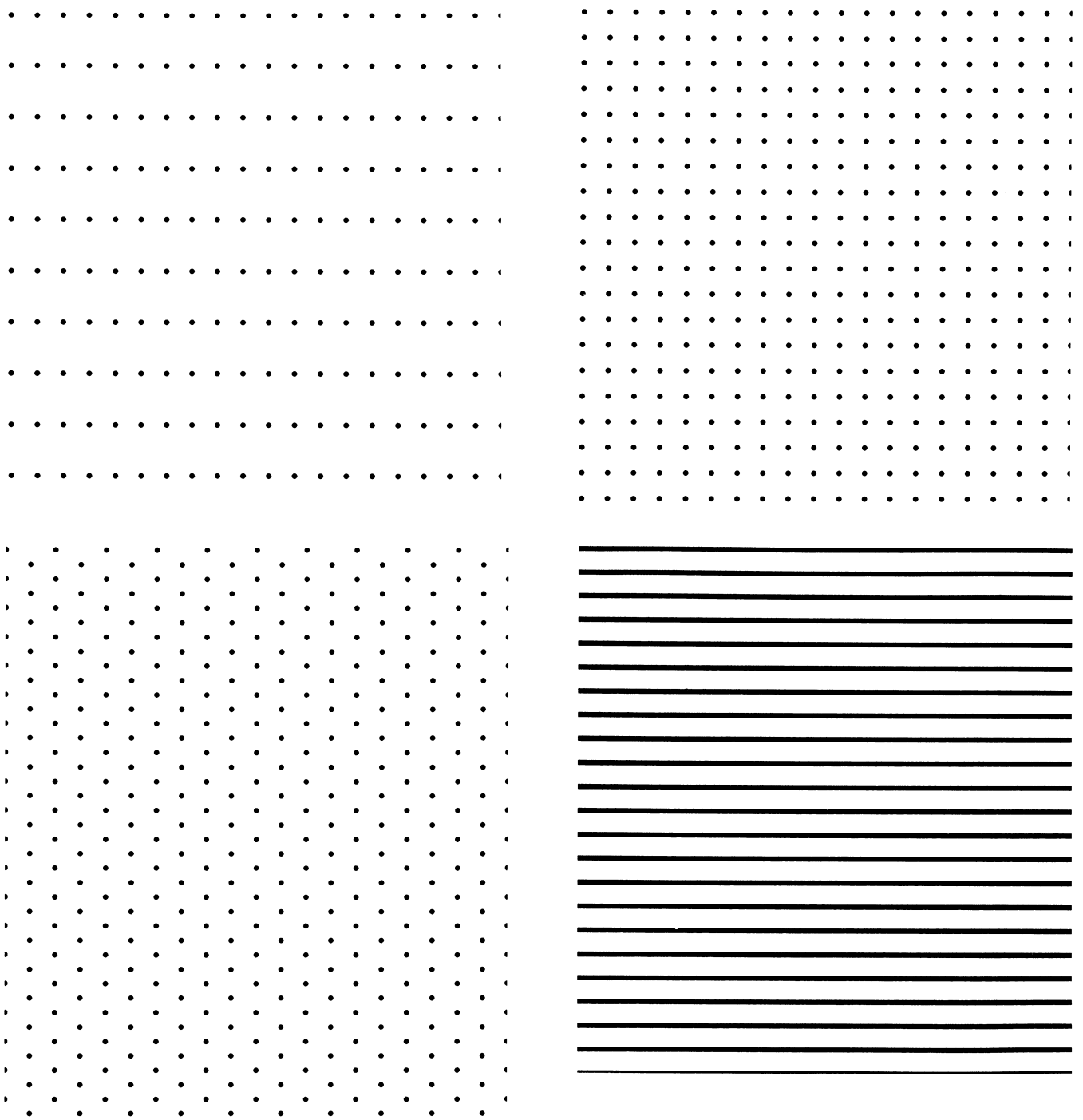

FIGURE 1. (a) A rectangular lattice, period 2. (b) A square lattice, period 4. (c) A hexagonal lattice, period 6. (d) Parallel lines, period 2.

3. DETERMINING THE RESOLUTION

Now that the visual devise has demonstrated the form of its underlying structure and we recognise it as a rectangular grid, we seek a way for the device to demonstrate the dimensions of the grid which it actually presents, i.e. to demonstrate its resolution.

Interference between two families of curves has the effect of magnifying any variations displayed by the families. By viewing a suitable picture and observing the interference caused by the interaction of the picture and the underlying rectangular lattice, we can use this magnification effect to estimate the lattice dimensions.

The simplest form of interference, that between two families of parallel lines with equal spacing λ and inclined at a small angle θ, is shown in Figure 4. Here the spacing λ is the perpendicular distance from the centre of one line to the centre of the next and the interference will show for any angle θ less than approximately 45° (Firby and Hubbard, 1990). The interference is again a family of parallel lines.

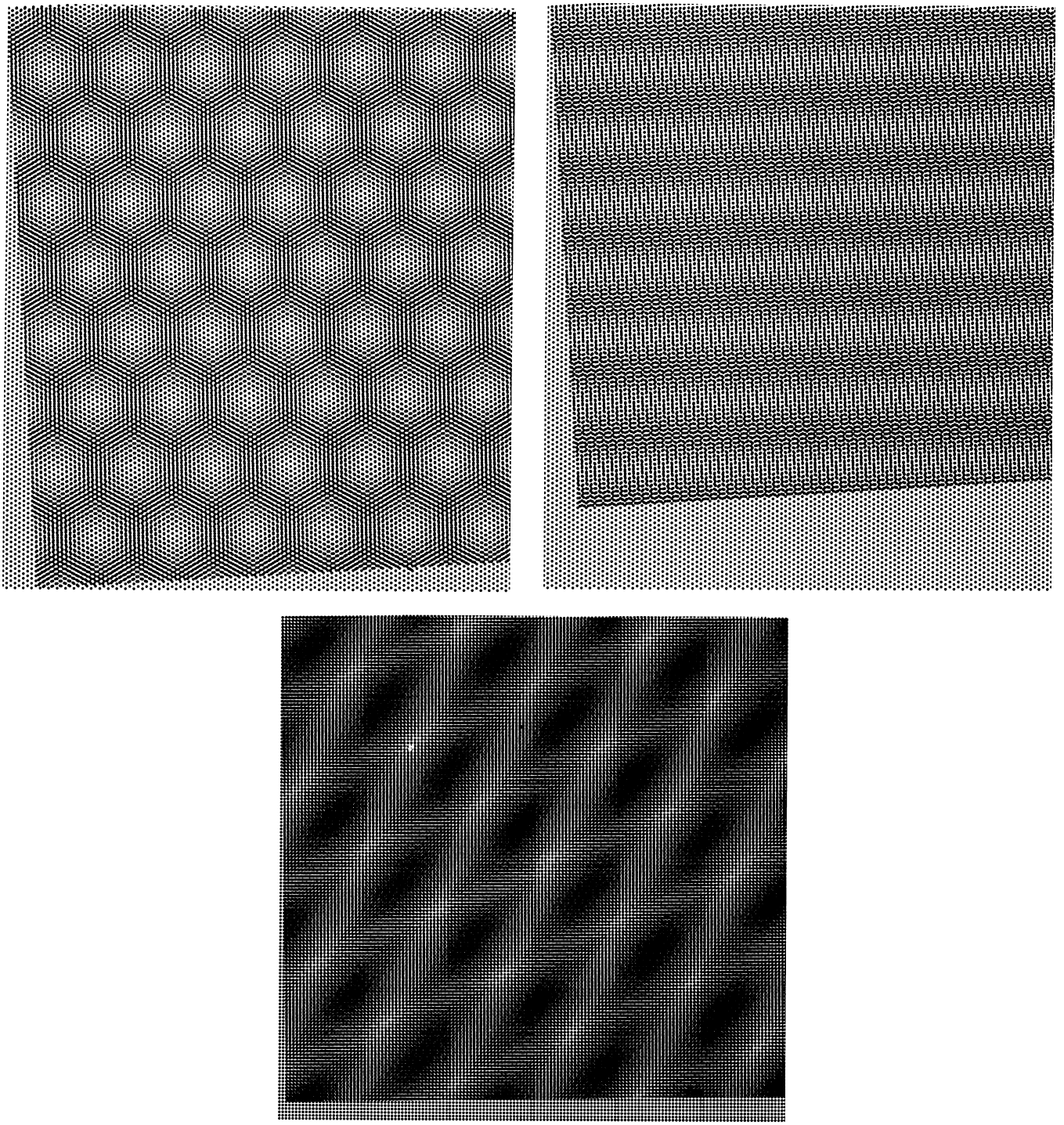

FIGURE 2. (a) A hexagonal lattice superimposed on a hexagonal lattice. (b) A hexagonal lattice superimposed on a square lattice. (c) A rectangular lattice superimposed on a square lattice.

In general if $\phi : U \to \mathbb{R}$ is smooth, where U is open in $\mathbb{R}^2$ and where y is a regular value of ϕ for each $y \in \phi(U)$ (i.e. $\phi(x) = y$ implies $\nabla\phi(x) \neq (0,0)$), then the set $\{\phi^{-1}(h) : h \in H\}$, where H is some suitable finite or countable 'indexing set', defines a family of curves. At $x \in \phi^{-1}(h)$ we define the *local spacing* at x, denoted by $\lambda(x)$, to be the arc length from x to $\phi^{-1}(h+1)$ along the orthogonal curve to the family through x. It has been shown (Firby and Hubbard, 1990) that $1/\|\nabla\phi(x)\|$ can be taken as an approximation to the local spacing at x and that this value is exact in the case of the parallel lines above.

For two superimposed families of curves described by the functions ϕ and ψ the spacing at a point determines the order of interference seen at that point (Firby and Hubbard, 1990). If the spacing of one family is no more than 1.5 times that of the second then the first order interference will be seen. This interference follows curves

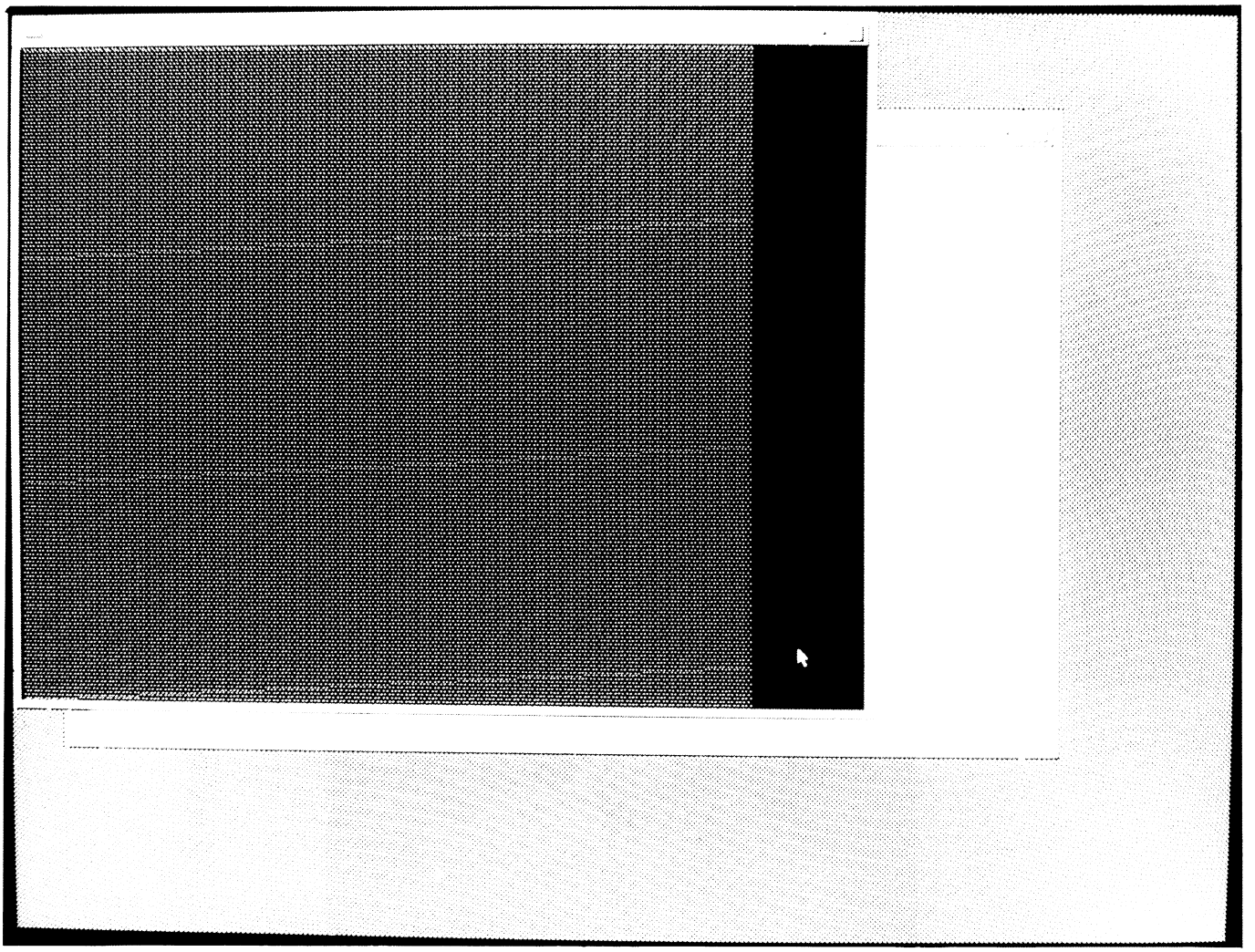

Figure 3. (a) A hexagonal lattice viewed on a monitor. (b) A square lattice, slightly rotated, viewed on a monitor.

in the direction of the shortest diagonals AB of the parallelogram shown in Figure 5, and is described by one of the functions $\phi \pm \psi$ (Firby and Stone, 1984).

If the spacing of one family is between 1.5 and 2.5 times that of the second then at that point second order interference will be seen, provided the crossing angle is small enough. This is the interference which follows curves in the direction of the shortest diagonal AB of the parallelogram shown in Figure 6 and is described by one of the functions $\phi \pm 2\psi$ or $2\phi \pm \psi$.

In a similar way nth order interference follows curves in the direction of the shortest diagonal of a parallelogram made up from one section of a ϕ curve and n sections of a ψ curve, or of one section of a ψ curve and n sections of a ϕ curve. This is described by $\phi \pm n\psi$ or by $n\phi \pm \psi$ and will be seen for sufficiently small angles when the spacing of one family is between $(2n-1)/2$ and $(2n+1)/2$ times that of the other family. Fractional orders of interference, e.g. the 3/2th order interference given by $3\phi \pm 2\psi$, can also occur but in normal conditions they are usually very weak. See Firby and Hubbard (1990) for an explanation of why this is so.

Now suppose we are given a family of parallel lines, described by

$$\phi(x, y) = \frac{y}{d} = t \ (t \in \mathbb{Z}),$$

where d is the fixed spacing, and a family of radial lines described by

$$\psi(x, y) = \frac{1}{\alpha} \tan^{-1}\left(\frac{y}{x}\right) = s \ (s \in \mathbb{Z}_m),$$

where ψ is defined on some suitable subset of $\mathbb{R}^2$ and where $\alpha = 2\pi/m$ is the angle between consecutive rays. Here $\mathbb{Z}$ denotes the set of integers and $\mathbb{Z}_m$ denotes the set of integers modulo m.

The effect of the superposition of these two families is shown in Figure 7. The variation in the spacing of the radial lines shows up in the appearance of several different orders of interference.

With a view to our application the picture of the radial lines has been started, at the left hand side of the picture, at the point where the local spacing is d and increasing. The first interference seen on the left is therefore the first order interference, and moving right the next strong

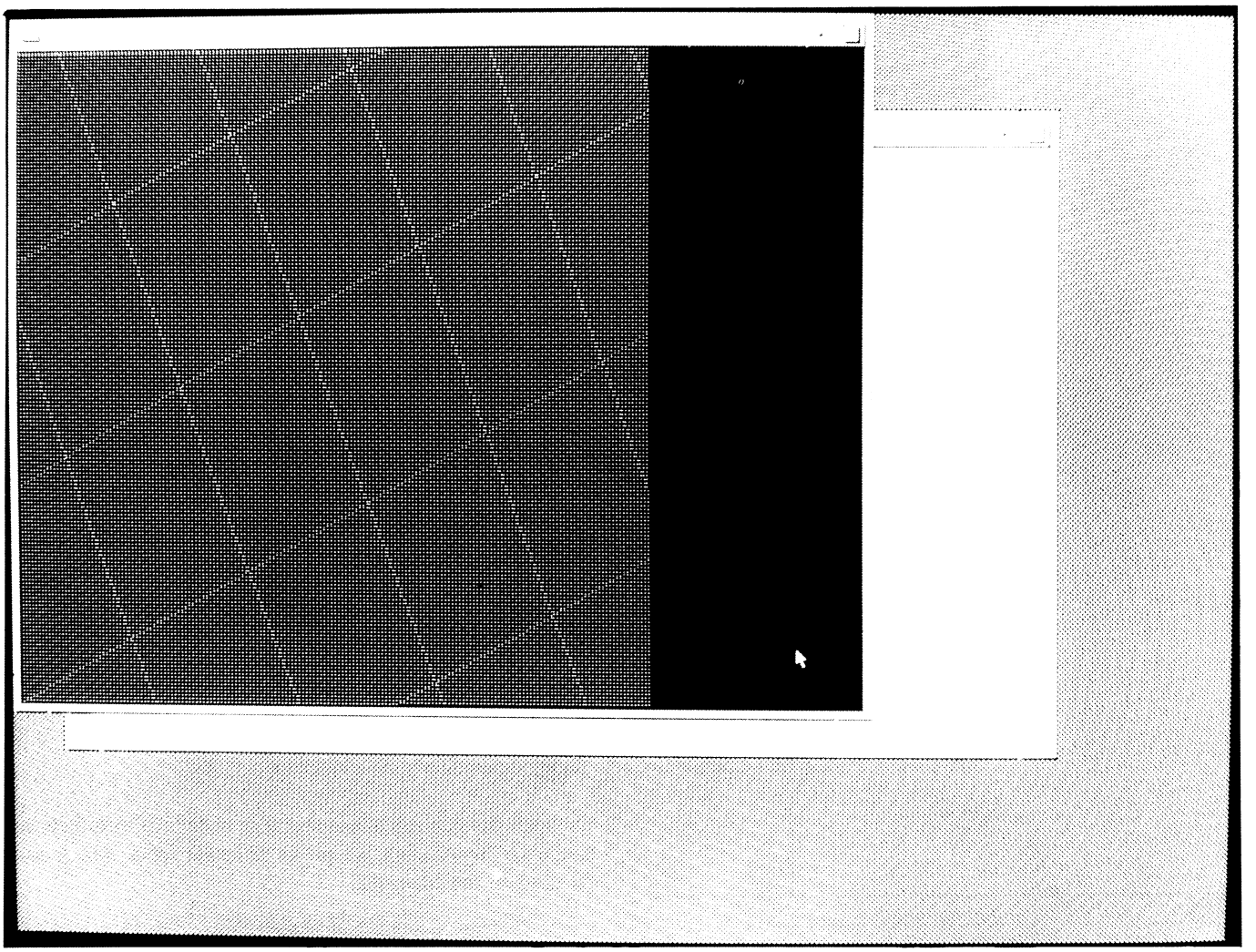

FIGURE 3. (Contd).

interference seen is the second order interference centered on the points where the local spacing of the radial lines is $2d$. Between these a faint 'ghost' of the 3/2th order interference can be seen and beyond the second order the even more faint forms of the 5/2th order interference can be seen.

From the above we see that the local spacing for ψ at (x, y) is given by

$$\frac{1}{\|\nabla\psi(x,y)\|} = \frac{\alpha(x^2+y^2)}{\|(-y,x)\|} = \alpha(x^2+y^2)^{\frac{1}{2}},$$

and so the points forming the centre of the nth order interference are given by

$$\alpha(x^2+y^2)^{\frac{1}{2}} = nd.$$

The point on the x-axis at the centre of the nth order interference is therefore given by

$$x = \frac{nd}{\alpha},$$

and so the distance μ between the centre of the nth order interference and the centre of the $(n+1)$th order interference is

$$\mu = \frac{d}{\alpha},$$

where α is the angle between consecutive radial lines and where d is the distance between consecutive parallel lines.

Now return to the investigation of the underlying rectangular grid structure of our visual device. This structure described horizontal and vertical lines whose distance apart, the resolutions of the device in the vertical and horizontal directions, we wish to measure.

Let the horizontal lines in the grid be described by the function $\phi(x, y)$ above, in which case the vertical resolution we seek is d. On the device view a picture of the family of radial lines given by $\psi(x, y)$. The observed picture will be completely filled from the centre of the radial lines up to the points where the local spacing is d. After this the interference shown in Figure 7 will appear, close to the x-axis. (Close to the y-axis the radial lines will be interfering with the vertical component of the underlying grid and so will give an estimate for the horizontal resolution.) Now if we measure the distance

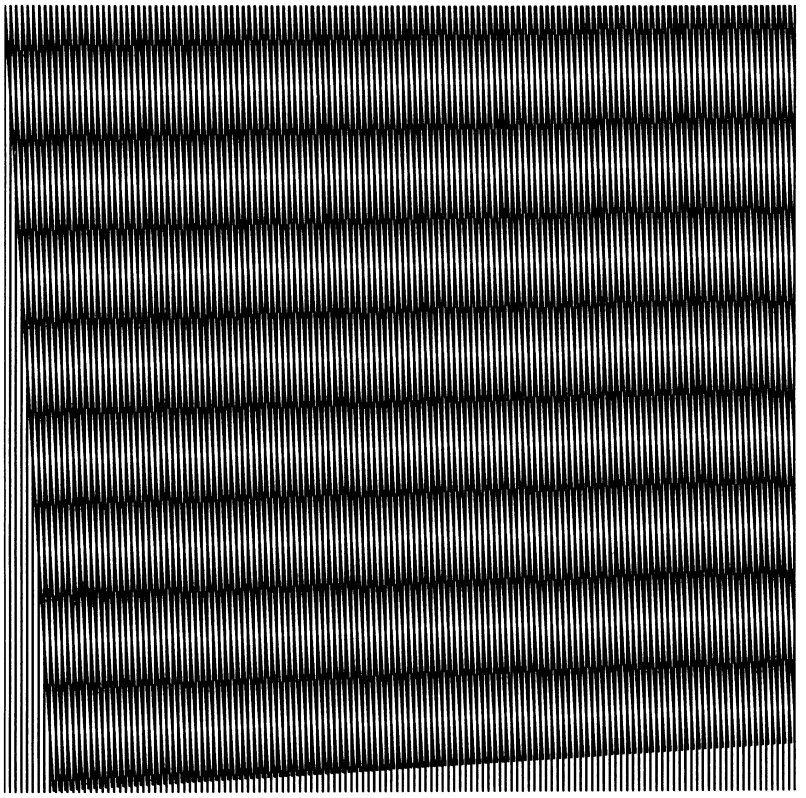

FIGURE 4. Parallel lines superimposed on a slightly rotated family of parallel lines.

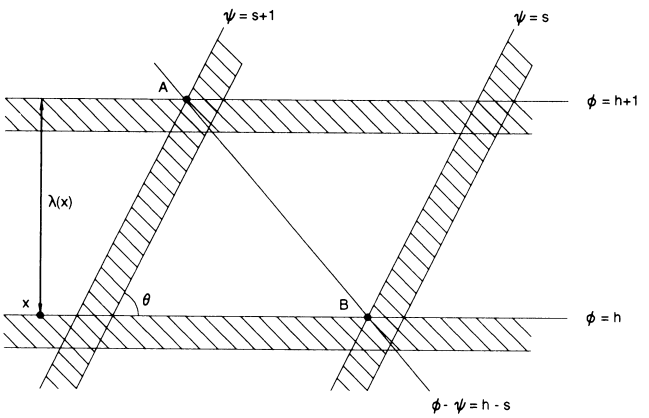

FIGURE 5. The position of the first order interference curves ϕ–ψ.

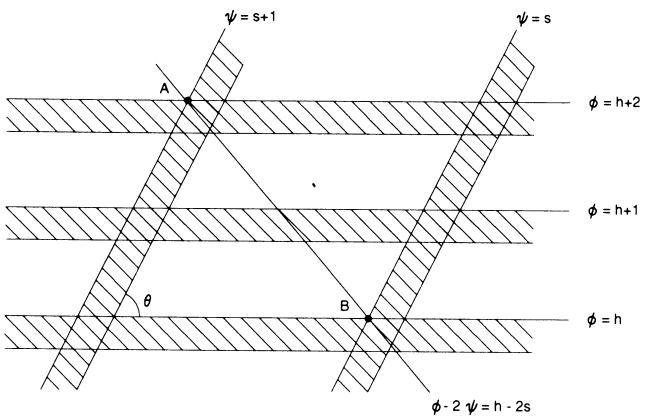

FIGURE 6. The position of the second order interference curves ϕ–2ψ

between the centres of consecutive orders of interference and take the average, we get an estimate for μ, which can be used in the formula

$$d = \alpha\mu$$

to estimate the vertical resolution d.

This procedure is demonstrated in Figure 8. The device is a 300 dots per inch laser printer and $\alpha = 2\pi/540$. The value μ was measured, to the nearest millimetre, between several centres of interference, and an average value of 7.25 mm obtained. This leads to a value of $d = 0.0844$ mm as an estimate of the vertical resolution.

The results of the above demonstration, and of similar experiments carried out on different devices, are listed in

TABLE 1. Resolution for some of the graphics devices tested

Device and Direction	*Device specification (mm)*	*Average μ (mm)*	*Estimated resolution (mm)*
300 d.p.i. laser (horizontal/vertical)	0.0847	7.25	0.0844
600 d.p.i. laser (horizontal/vertical)	0.0423	3.57	0.0415
Console type 1 (horizontal/vertical)	0.288	26.5	0.308
Console type 2 (horizontal)	0.244	23.0	0.268
Console type 2 (vertical)	0.244	22.0	0.256
Console type 3 (horizontal/vertical)	0.282	22.5	0.262

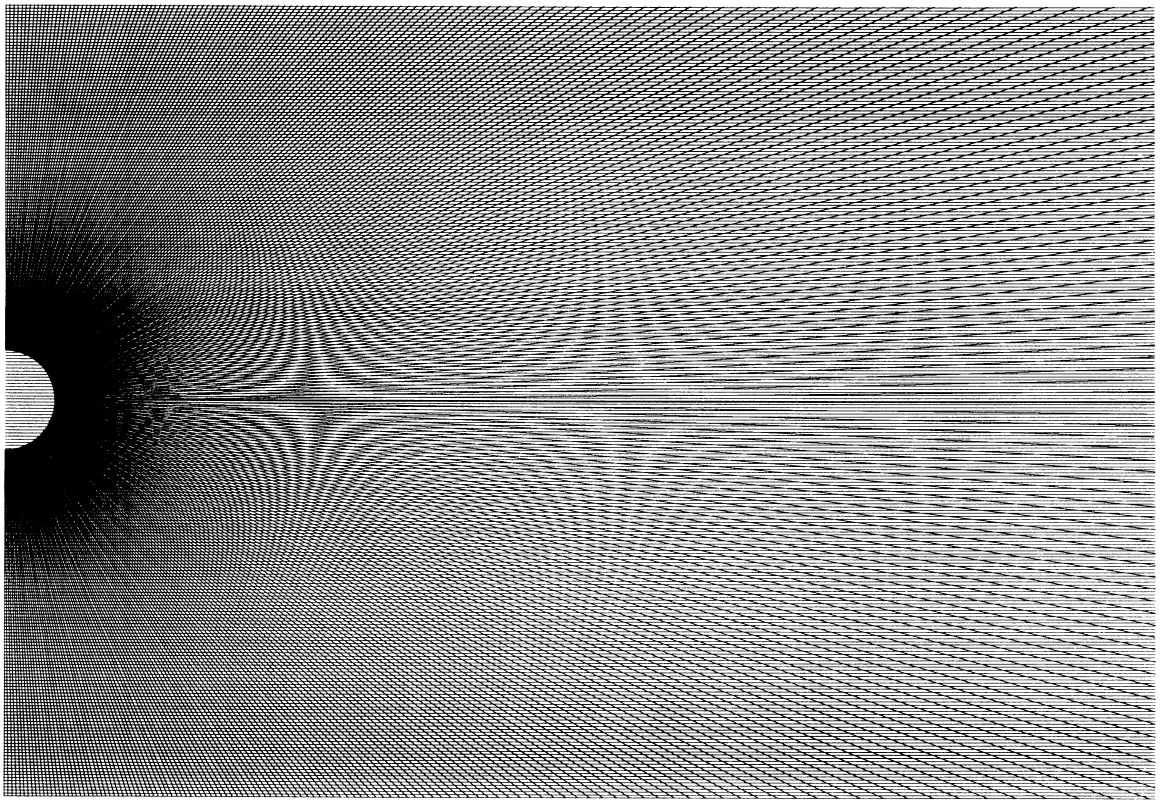

FIGURE 7. A family of radial lines superimposed on a family of parallel lines.

Table 1. In each cause the value μ was simply measured with a ruler to the nearest millimetre, α was taken as $2\pi/540$ and the resulting value for d was compared with the resolution obtained from the device specification. In the case of the laser printers, accurate machines which seem to be accurately set, our estimate is within 2% of the device specification. We believe that this is the sort of accuracy that this, apparently crude measurement

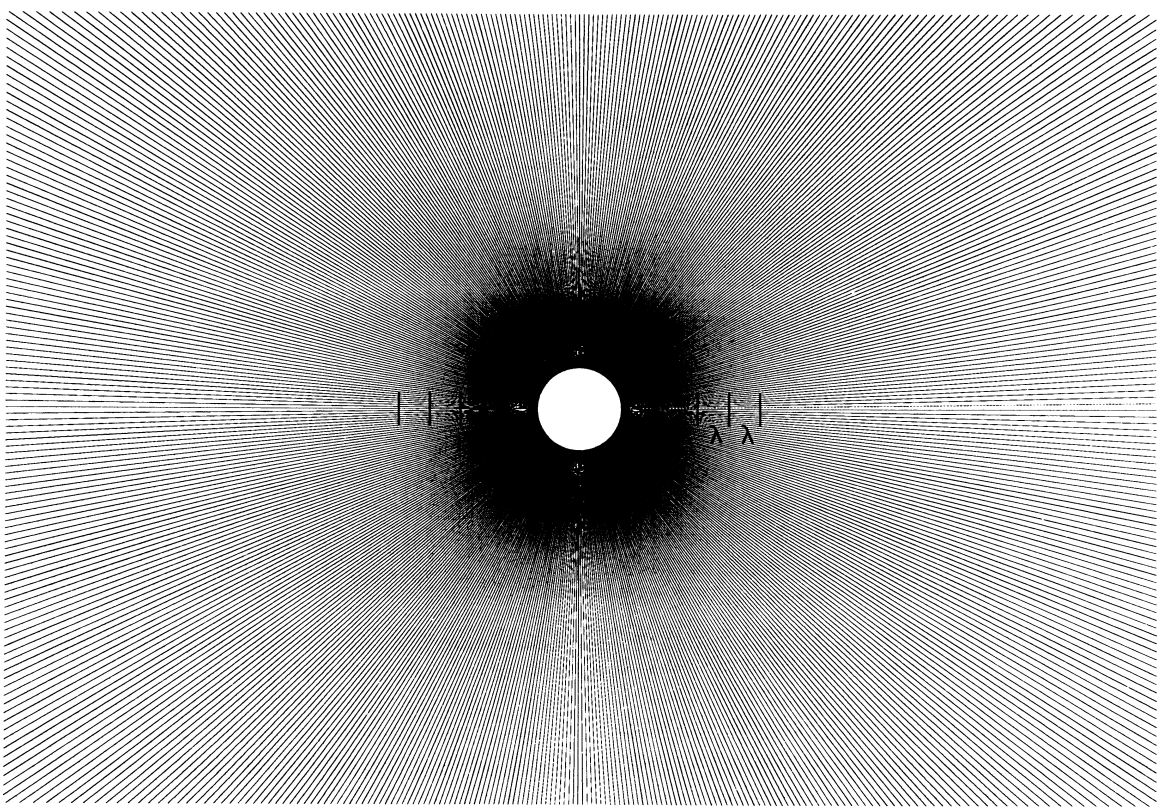

FIGURE 8. A family of radial lines displayed by a laser printer.

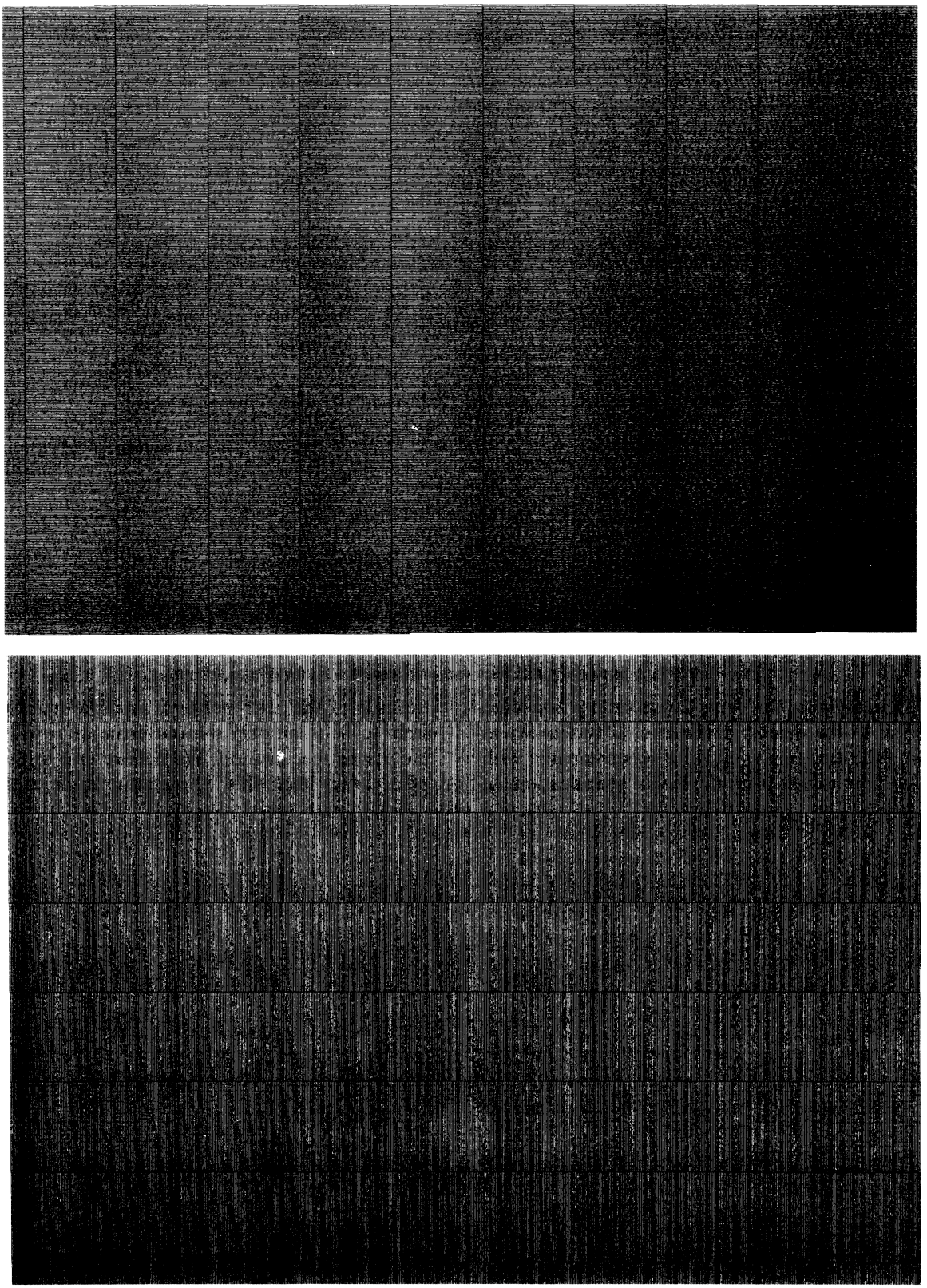

FIGURE 9. A family of parallel lines displayed by a laser printer. The spacing is four times the estimated resolution: (a) the lines are drawn at a slight angle to the horizontal and (b) the lines are drawn at a slight angle to the vertical.

by ruler, produces for the resolution of the final image. The estimates for the console resolutions varied by up to 9% from the device specification and this would appear to be mainly caused by a slight inaccuracy in the setting up of the screen width and height by the engineer. Adjustment based on the interference pattern would appear to be more accurate than setting screen width and screen height.

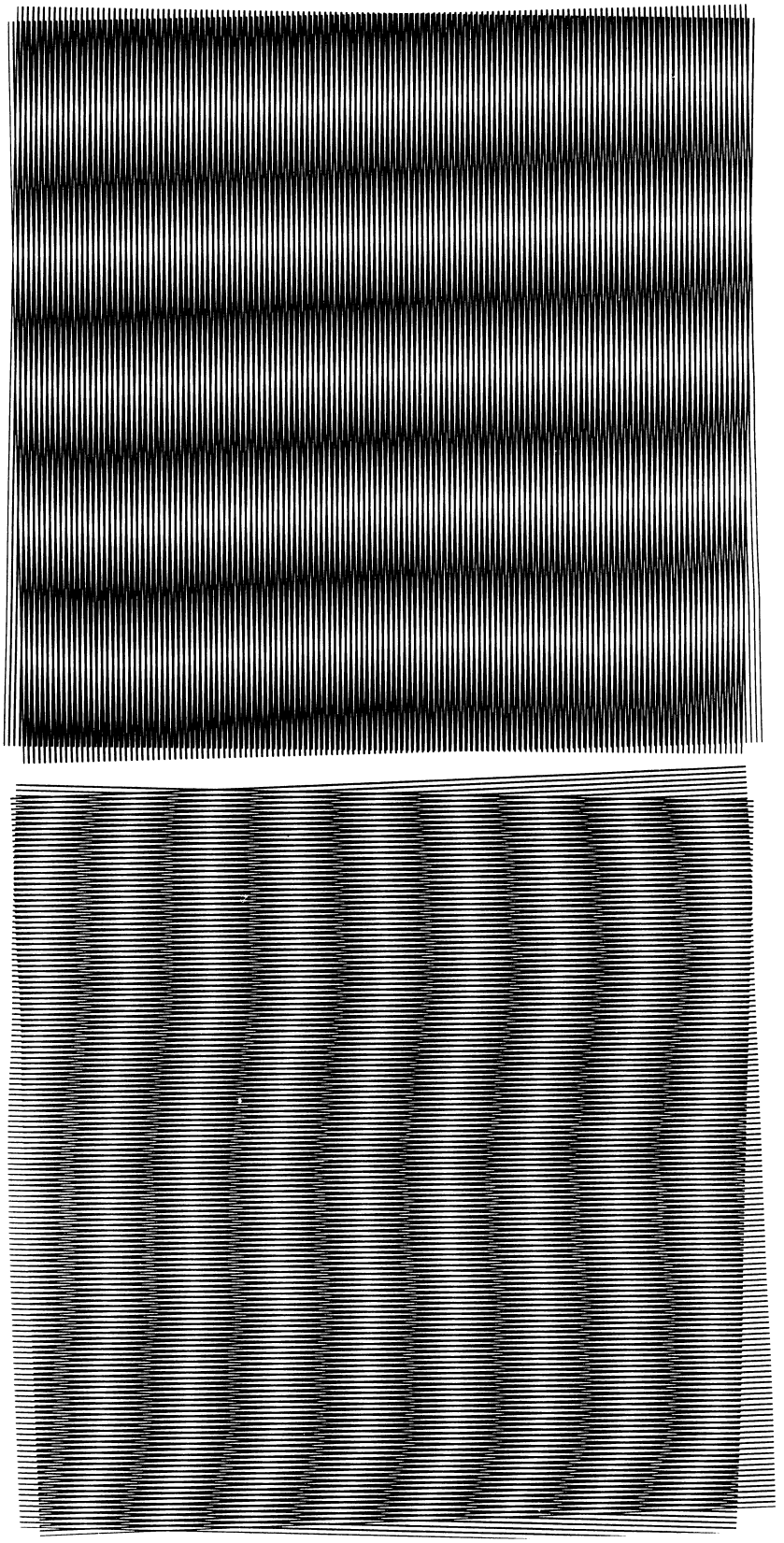

FIGURE 10. Displaying the distortion in a photocopier. Parallel lines are photocopied and then the same family overlayed at a slight angle. (a) With the lines vertical. (b) With the lines horizontal.

The consoles of type 2 in particular, at this University, all have the same variation of almost 5% between the estimated horizontal and vertical screen resolutions. They all appear to have been set at source with the same fault!

4. TESTING THE STRUCTURE

Finally, the knowledge of the geometry of the underlying grid structure and its dimensions can be used to test the

accuracy of this structure. Asking the device to display a family of lines of spacing say four times the resolution and at a small angle to the horizontal should produce as interference parallel lines at a small angle to the vertical. Any horizontal distortion or displacements in the underlying structure should then be magnified in the interference. Figure 9(a) shows this test applied to the 300 d.p.i. laser printer where the angle chosen is $\pi/1000$. Figure 9(b) shows the same test for vertical distortion or displacement. It can be seen that the machine displays remarkable accuracy.

Compare this with a similar test applied to the overlay operation of a photocopier. In Figure 10(a) a family of parallel lines has been photocopied and then the same family overlayed at a slight angle. The interference shows the considerable distortion produced by the machine in say the y-direction. The same process applied to the picture rotated through $\pi/2$, seen in Figure 10(b) shows that the device produced much less distortion in the x-direction. Figures 10(a) and (b) can be compared with Figure 4, the same picture displayed through the laser printer.

REFERENCES

Amidror, I. (1991). The moiré phenomenon in colour separation. In Morris, R. and André, J. (eds), *Raster Imaging and Digital Typography II*, pp. 98–119. Cambridge University Press, Cambridge.

Bryngdahl, O. (1976) Characteristics of superposed patterns in optics. *J. Optic Soc. Am.*, **66,** 87–93.

Coxeter, H. S. M. (1969) *Introduction to Geometry*, Wiley, New York.

Firby, P. A. and Stone, D. J. (1984) Interference patterns and two-dimensional potential theory. *IMA J. Appl. Math.*, **33,** 291–301.

Firby, P. A. and Hubbard, S. J. (1990) Moiré separations. *IMA J. of Appl. Math.*, **45,** 49–80.

Harthong, J. (1981) Le Moiré. *Adv. Appl. Math.*, **2,** 24–75.

Hoggar, S. G. (1992) *Mathematics for Computer Graphics*. Cambridge University Press, Cambridge.

Kendig, K. M. (1980) Moiré phenomena in algebraic geometry: polynomial alternations in $\mathbb{R}^n$. *Pacific J. Math.*, **89,** 327–349.

Steinbach, A. and Wong, K. Y. (1979) *An Understanding of Moiré Patterns in the Reproduction of Half-tone Images*. IEEE Computer Society, Chicago.

Tollenaar, D. (1957) *Moiré Pattern in Printing*, pp. 3–18. Research and Engineering Council of the Graphics Arts Industry, Washington.